

# FLOW DISTRIBUTION IN A HYDRAULIC HEADBOX

Lu Hua, Eric Bibeau <sup>\*</sup>, Pingfan He, Martha Salcudean and Ian Gartshore  
Department of Mechanical Engineering, The University of British Columbia, Vancouver, BC V6T 1Z4  
<sup>\*</sup>Process Simulations Limited (PSL), #204, 2386 East Mall, Vancouver BC V6T 1Z3 (www.psl.bc.ca)

## ABSTRACT

Flow modeling of a hydraulic headbox with a tapered manifold, a large array of diffuser tubes, and a symmetrical slice has been numerically investigated. Numerical methods for turbulent flows in complex three-dimensional geometries have been used with body-fitted co-ordinates and non-orthogonal grids. The complete flow field in the manifold, diffuser tubes, and slice have been simultaneously calculated. The average velocity in each of the diffuser tubes is non-uniform in both the cross-machine direction (CD) and across rows of tubes. The effect of the recirculation ratio is shown to significantly affect the flow distribution across the diffuser tubes, especially in the region near the exit of the manifold. The cornering of the flow as it enters each diffuser tube causes a significant recirculation zone near the front wall of each tube. The exit flow from each diffuser tube is shown to be highly non-uniform with a significant degree of interaction as the flow proceeds into the slice. The converging section reduces and stretches the flow structures, producing a more uniform flow at the exit. The present study is part of a larger effort to develop advanced computer models for predicting complex flows in headboxes, and serves as an important step for predicting fluid-fiber interactions to provide paper manufacturers better control over fiber orientation, fiber distribution, and sheet properties.

## INTRODUCTION

In a hydraulic headbox, stock is admitted in a tapered manifold and flows across the width of the machine with a portion of the stock being recirculated to prevent a pressure build-up at the manifold exit. An array of small diffuser tubes connects the manifold to the slice, which produces a free jet that impinges on the forming section. In order to supply well dispersed stock containing a constant percentage of fibers to all areas of the sheet-forming section, and because fibers in headboxes tend to form flocs rapidly, removal of flow non-uniformities and the creation of high intensity turbulence is required in headbox designs. Variation of fiber orientation and basis weight profiles in the cross-machine direction are dependent on the headbox design and operation mode. Eventually, headbox designs may be flexible enough to provide paper manufacturers the ability to select sheet properties they require with minimal changes to the headbox. This will require a better control of fiber distribution emanating from the headbox, the prevention of flow non-uniformities originating in the headbox in the machine direction (MD) and cross-machine direction, and a method to control MD/CD ratios over a wide range. To achieve this goal, a detailed understanding of fluid flow within the entire headbox and fluid-fiber interaction is required.

Optimization of the manifold, turbulence generating section, and slice have been obtained through experimentation, simplified analysis, and more recently using numerical analysis. The analysis and design of headbox manifolds, for example, was traditionally based on a one-dimensional energy balance of the flow inside the manifold [1], and design guidelines to obtain a uniform flow distribution at the slice exit were formulated [2]. Until recently, the complexity of the geometry and the three-dimensional turbulent flow field occurring in headboxes did not allow for a complete flow calculation. Therefore, there have been few numerical calculations of flows in headboxes. Syrjälä *et al.* [3] investigated an actual headbox manifold but not the diffuser tubes. Jones and Ginnow [4] calculated flow parameters in a straight channel diffuser in three dimensions and in a Beloit experimental headbox in two dimensions. Predictions compared favorably with available experimental data. The authors recommended further validation of the parameters in the  $k - \epsilon$  model and investigation of the eddy size variation in manifolds. Shimizu and Wada [5] calculated a generic headbox using a body-fitted coordinate system. The flow distribution in the manifold was investigated in two dimensions and the flow area reduction was calculated in three dimensions with assumptions of periodicity. The jets from the diffuser tubes were modeled in three dimensions using calculation results obtained for a single tube. Hämäläinen [6] linked two-dimensional models of the manifold, the turbulence generating section, and the slice using finite element. The pressure drop in each tube was assumed to be that of a single tube using the homogenization technique. The model was then applied to the optimization of a headbox [7]. Separate three-dimensional models of the manifold and of the slice have been performed by Lee and Pantaleo [8] to investigate various effects of headbox control devices on flow characteristics and fiber orientation. Aidun [9, 10] investigated secondary flows in the slice section.

Previous numerical studies for the calculation of the flow distribution from the manifold either ignore the diffuser tubes, model tubes in two-dimension, or assume single tube behavior. These studies may not model the flow non-uniformities existing across the diffuser tubes caused by (1) headbox design problems and design compromises resulting in a deviation from the desired pressure profile across the manifold, (2) variation in geometry of the tubes, and (3) change in the pressure drop across identical tubes caused by velocity variation along the manifold [2]. In addition, a detailed three-dimensional model that can calculate the pressure loss at the inlet of the turbulence generating section due to friction losses, losses due to the fluid turning around the corner, and flow leakage out of laterals [1] has yet to be demonstrated. Numerical modeling of the slice section does not in general incorporate the exact flow field emerging from the turbulence generating section. The flow to the inlet of the slice contains local flow non-uniformities and flow variations in the paper thickness direction (PD) and cross-machine direction, creating flow structures at the beginning of the slice. To effectively control the flowmechanics of a headbox, calculations of flow quantities—including velocity distribution, vorticity, strain rate, pressure, and turbulence characteristics—are required to understand fluid-fiber interactions and quantify the influence of the manifold, turbulence generating section, and slice on the distribution and orientation of fibers as they exit the slice and form a free jet. The object of this study is to demonstrate the predictive ability of a three-dimensional headbox model which can be used to trouble-shoot existing headboxes, evaluate proposed retrofits, compare headbox designs, predict the influence of control devices and operation modes on flow behavior, and serve as an important step for predicting fluid-fiber interactions.

### **HEADBOX NUMERICAL MODEL**

The three-dimensional incompressible Reynolds averaged Navier-Stokes equations are solved. Turbulence closure is obtained by the use of the standard  $k - \epsilon$  model with the wall function treatment. A finite volume method in conjunction with general curvilinear grids is used. A staggered grid arrangement in which the velocity components are located on the control-volume surfaces and pressure is located in the control-volume center is used. The physical tangential velocity components are used as the primary velocity variables in the momentum equations. Discretization is done by directly using the coordinate-invariant governing equations. The coordinate-invariant governing equations are integrated directly in the physical control volumes. The discrete governing equations are obtained by expressing the resulting surface fluxes using the discrete velocity values and the grid physical geometric quantities, which include the volumes, the surface areas and surface normal directions of the physical control volumes. These physical geometric quantities can be calculated according to certain rules in order to satisfy the geometric conservation laws. This method is more desirable for non-smooth grids since the coordinate derivatives, which are not well-defined on an irregular grid, are avoided and all the formulas have clear physical meaning. A domain segmentation method is also implemented. The method divides the domain of interest into different flow regions. For instance, the headbox is decomposed into the tapered duct (1 to 4 segments), the diffuser tubes (32 to 960 segments), and the slice (1 or 2 segments). A solution is obtained by repeatedly applying a single-domain solution solver to all the segments, and cycling through all the segments until the residuals are sufficiently small. Efficient communication between the segments is established to achieve fast convergence by appropriately transferring data between adjacent segments for each iteration. Validation cases for manifold applications can be found in Reference [11]. The detailed formulation of the code, developed at the University of British Columbia, can be found in Reference [12].

### **HEADBOX PHYSICAL MODEL**

The "generic" headbox geometry used in this study is shown in Figure 1. The headbox avoids resemblance to a commercial product but still retains similar features of a commercial headbox. The headbox manifold consists of a tapered rectangular duct 4000-*mm* wide with the largest rectangular cross-section measuring 600 *mm* by 266 *mm* and the smallest 152 *mm* by 266 *mm*. The inlet duct diameter is 457 *mm* and the outlet duct diameter is 86 *mm*. Each tapered diffuser tube is 275-*mm* long with an inlet square cross-section 13 *mm* in width and an outlet square cross-section 31 *mm* in width. The square outlet diffuser tubes are separated by a 2 *mm* wall on all sides. There are 8 rows of 120 diffuser tubes comprising the turbulence generating section connecting the manifold to a calming section 100-*mm* long immediately followed by a symmetrical slice 760-*mm* long.

The flow in the headbox is assumed steady and incompressible and turbulence is modeled using the standard  $k - \epsilon$  model, including the slice section even though some studies suggest that secondary flows due to anisotropy is important [9, 10]. Our own numerical calculations of the slice using different non-linear  $k - \epsilon$  turbulence models has shown these secondary flow are present, but are confined to a small region near the side walls of the slice and do not dominate the flow field.

Taking advantage of flow symmetry, only half of the flow domain is calculated: half of the manifold duct, the first four rows of diffuser tubes, and half of the slice section. The grid used contains  $544 \times 13 \times 13$  grid nodes for the manifold,  $7 \times 7 \times 9$  grid nodes for each diffuser tube, and  $961 \times 33 \times 16$  for the slice. A finer grid was also used

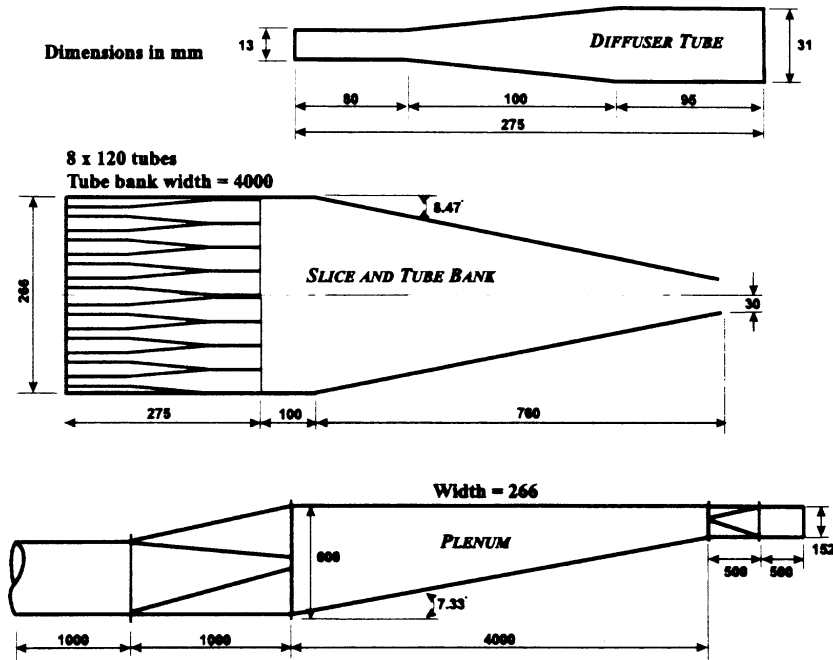


Figure 1: Diagram of hydraulic headbox used in the present study: rectangular cross-sectional tapered manifold, 960 tapered diffuser tubes (8 rows by 120 columns), and symmetrical slice without lip

containing  $18 \times 18 \times 19$  grid nodes for the first 8 columns of diffuser tubes and  $161 \times 81 \times 31$  for the partial slice. The grid is generated using a combination of an elliptic grid generation method and an algebraic generation grid method. Grid refinement of the manifold upstream of the inlet of the diffuser tubes will be reported in a separate study. Some of the grid independent study results have been reported in Reference [11].

Different types of boundary conditions are used: inlet velocity for the headbox entrance, outlet velocity to model the recirculation flow; zero-slip wall condition to model all headbox internal surfaces; symmetric boundary conditions with zero flux and a free-slip condition to model the symmetry plane; and an imposed shear-stress caused by the area change of the slice at the slice outlet. Results were obtained using water and an inlet manifold flow velocity of  $5.8 \text{ m/s}$ .

### MANIFOLD FLOW DISTRIBUTION

The velocity ratio, defined as the ratio of the average velocity from a tube by the average velocity if the flow emanating from all the diffuser tubes was uniform, is shown in Figure 2a for a recirculating ratio of 25%. The results are shown for each of the 4 rows of tubes simulated. The velocity distribution varies in both the cross-stream direction and the paper

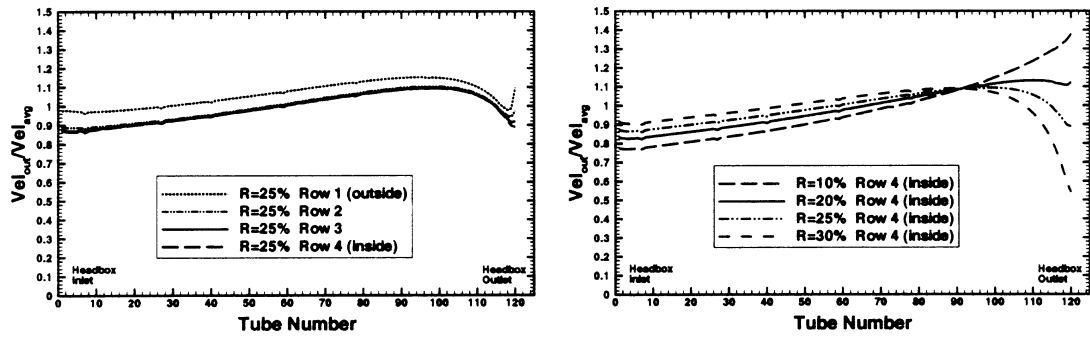


Figure 2: (a) Average flow emanating from tube rows 1 to 4 for a recirculation ratio of 25%, and (b) Average flow emanating from the fourth (inside) diffuser tube row for recirculation ratios 10%, 20%, 25%, and 30%

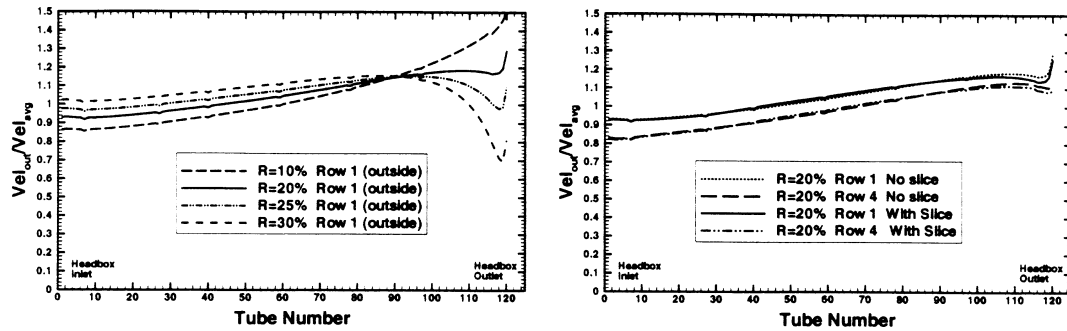


Figure 3: (a) Average flow emanating from the first (outside) diffuser tube row for recirculation ratios 10%, 20%, 25%, and 30%, and (b) Average flow emanating from the first and fourth diffuser tube rows with and without the slice included in the numerical model

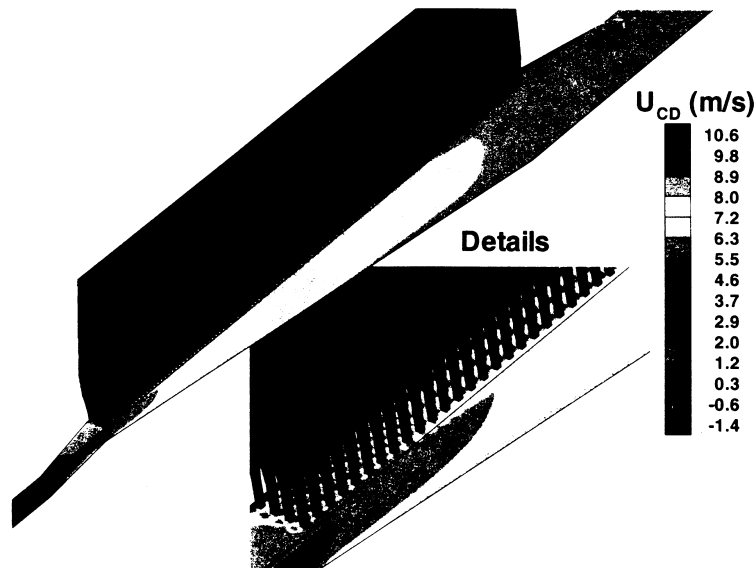


Figure 4: Velocity distribution in the cross-machine direction of half of the headbox

thickness direction. The flow variation across rows only occurs for the row that is closest to the outside wall of the manifold. There is no flow variation for the other three rows simulated. This variation is typical of some commercial headboxes as these tend to have tapered side walls upstream of the turbulence generating section causing more fluid to flow in the first row of tubes located closest to the manifold wall. For a rectangular manifold with straight side walls, more fluid flows in the first row of tubes as the side wall may act as a flow straightener, funneling the flow into the first row. In addition, it is postulated that less energy leakage occurs compared to the other rows as the flow moves between local areas of vorticity occurring at each tube entrance. This effect would override the momentum deficiency created by the boundary layer at the wall.

The variation in the cross-stream direction is because the manifold exit height was set to a larger dimension than that predicted by one-dimensional calculations. The distribution or signature of the manifold exhibits some of the typical behaviors near the entrance and exit of the headbox. This variation is caused by the approach flow to the turbulence generating section and the exit geometry causing variations in pressure upstream of the tubes. At the entrance, the flow entering the first few columns of tubes will experience different flow conditions and different shear stresses close to the tubes inlet. Near the exit of the headbox, flow non-uniformity out of the diffuser tubes is caused by the recirculating flow exiting the tapered channel and streamlines converging into a circular pipe creating pressure variations. This aspect is shown in Figures 2b and 3a, which show the flow distribution for the first and fourth rows and for recirculation ratios of 10%, 20%, 25%, and 30%. If the recirculation ratio is too low, a pressure build-up at the exit occurs and more flow will be forced through the last few columns of tubes. When the recirculation ratio is set to high, the pressure will decrease and less flow will pass through the tubes. The first row corresponding to the row on the outside of the turbulence generating section has a slight kink for recirculation ratios greater than 10%. This kink is a result of the pressure build occurring as the flow approaches the recirculating pipe. The signature of the manifold will deteriorate at velocity

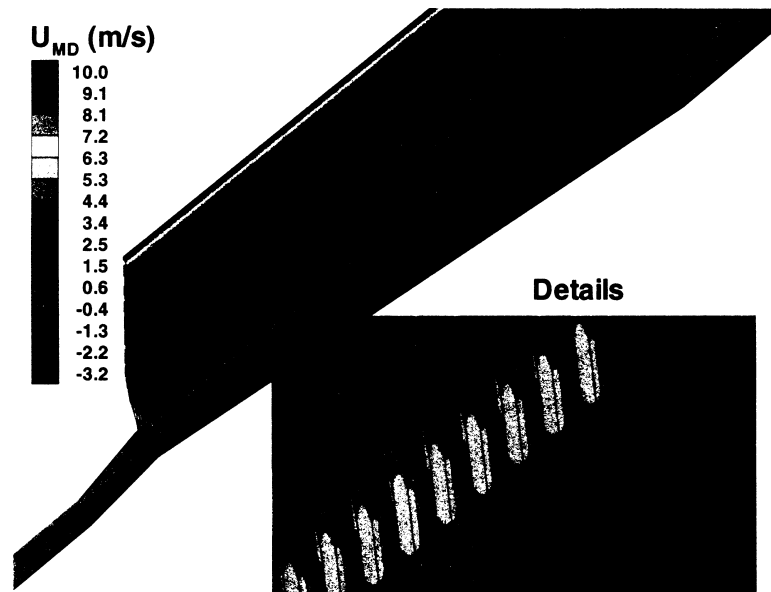


Figure 5: Velocity distribution in the machine direction of half of the headbox

outside the design range. The flow distribution from the slice can, to some degree, correct the flow non-uniformity but this will create flows in the cross-machine direction and influence fiber angle distribution. For the 10% and 20% recirculating ratios, the mean outlet diffuser tube velocity decreases near the manifold exit, as the pressure across the diffuser tubes decreases.

In general, the signature of the manifold was found to be relatively insensitive to the turbulence bank geometry [13] and insensitive even to the boundary conditions imposed. Figure 3b compares the signatures for a 20% recirculation

ratio for rows 1 and 4 for the complete calculation of the headbox and for a calculation where the slice was not modeled and a zero gradient condition was imposed at the exit of the turbulence generating section. Although this later condition is not realistic, the signature compares favorably well with the complete headbox calculation. This result is a consequence of the parabolic nature of the flow where local flow conditions are relatively insensitive to conditions downstream.

Figures 4 to 6 show the velocity in the cross-machine direction, the velocity in the machine direction, and the pressure distribution in half of the headbox and for a recirculation rate of 25%. The velocity in the cross-machine direction in the manifold, Figure 4, increases as the flow proceeds toward the exit. The flow gradients in the slice are caused by the uneven flow distribution produced by the manifold which may lead to possible variation in fiber orientation in the cross-machine direction. The velocity in the machine direction, Figure 5, is more uniform and tubes appear at first glance to behave in identical ways. A closer look at individual tubes would reveal small variations in velocity magnitude and direction, but not in flow structures. The pressure in the manifold is fairly constant except near the exit where a pressure decrease is observed as the flow proceeds through the recirculation pipe, as shown in Figure 6. It is this pressure change at the basis of the flow tubes which causes the flow variations shown in Figures 2 and 3. Figure 7 shows the flow distribution at three cross-sections of the rectangular manifold. There is no apparent recirculation region as the flow proceeds upwards due to the presence of the tapered bottom wall.

### FLOW NON-UNIFORMITY IN DIFFUSER TUBES

Grid refinement of the first section of the headbox was performed for the first 8 tube columns and the 4 rows modeled, including the adjacent slice section. To properly take into account the flow cornering into the diffuser tubes, the flow into each of the 32 tubes was obtained from the complete flow calculation of the headbox. Figure 8 shows the velocity vectors and pressure contours for a typical tube. The velocity vectors are strongly skewed towards the back wall of the tube. This is even more evident as the flow proceeds through the tube before the expansion occurs. During the expansion, an adverse pressure gradient causes the flow to recirculate on the front wall of the tube. This behavior is characteristic of all 960 diffuser tubes. After the expansion, the flow begins to reattach and all velocities in the machine direction become positive. The flow exiting the tubes is highly non-uniform, with the flow being skewed towards the headbox inlet and more fluid flowing towards the back end wall of the tube. Constant velocity planes in the machine direction and cross-machine direction are shown in Figure 9a. The results show that the largest velocities are along the back end wall of the tube.

The flow into the tubes was recalculated using a uniform inlet velocity at the tube base to simulate hydraulic headboxes that have a flow straightener tube bank before the turbulence generators, and to check the assumption of using uniform flow into a tube for a numerical model. Figure 9b compares the velocity streamlines for the case where

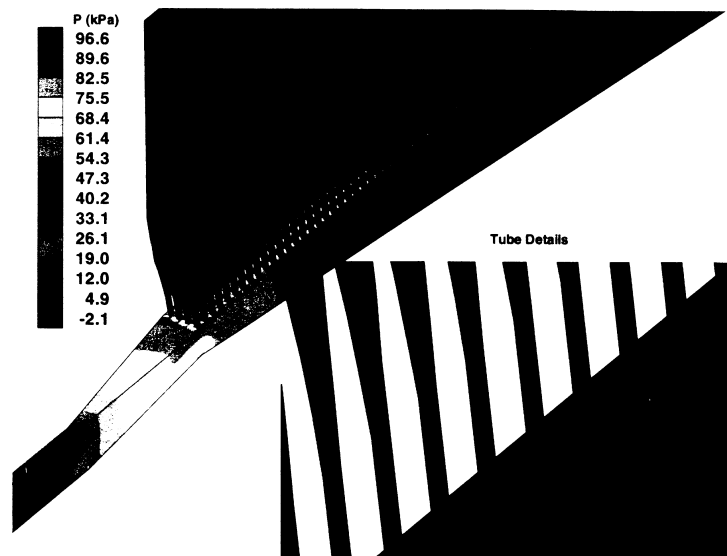


Figure 6: Pressure distribution of half of the headbox near the exit

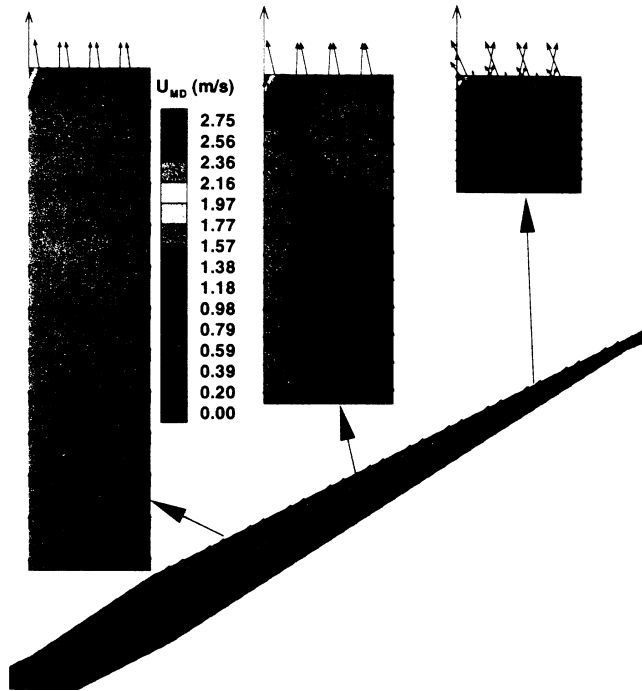


Figure 7: Flow distribution at three cross-sectional rectangular planes in the tapered manifold

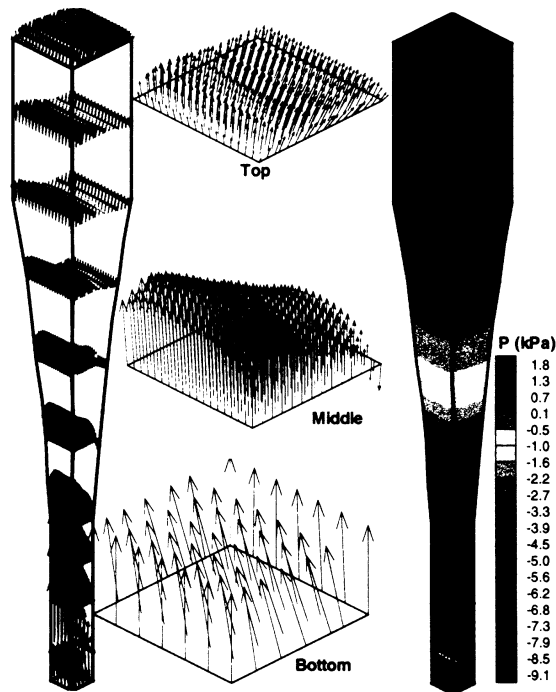


Figure 8: Velocity vectors and pressure distribution in one of the diffuser tubes

the velocity inlet is calculated by the headbox model, thus accounting for the cornering of the flow, and for the case where a uniform velocity at the inlet is imposed. For each case, the results are shown for a plane near the edge of the tube and for a plane in the middle of the tube. For the normal inlet resulting from properly modeling the cornering of

the flow, the recirculation zone previously described is shown to be stronger near the edge plane as compared to the mid plane because of the presence of the sharp corner. Streamlines show no recirculating region in the mid plane when assuming a straight velocity profile at the inlet of the tube. Two small recirculating regions occur near the edge plane for this case, as expected. The impact on fiber motion in light of the recirculation regions must be evaluated as flow detachment will produce unsteady fluid motion and pressure fluctuation which may not be desirable. The recirculation zone may distribute the fibers more randomly on one side of the tube, causing a non-uniform fiber distribution across the square cross-section of the tube exit.

### CONVERGING SECTION

Because the flow exiting the diffuser tubes is highly non-uniform and we are eventually interested in determining the fiber distribution and orientation, it is important to properly model the correct flow condition entering the slice and the turbulence history of the flow up to that point. Figure 10 shows the flow field for a section of the slice connected to the first 8 columns and 4 rows of tubes, as discussed in the previous section. There are 32 tubes connected to this slice region. Velocity vectors at vertical planes in the calming section, mid slice and slice exit are shown with pressure contours. As can be seen in this figure, the flow is very non-uniform emanating from the turbulence generating section. Note that there is a small region between each diffuser tube caused by the thickness of each tube wall where the velocity in the machine direction is zero at the wall. The flow must slightly expand to fill this region. Interaction between each flow structure, having a size of the order of the tube width, interact and form a secondary flow in the slice. These flow structures are dominant and significant when compared to smaller structures created in the wall boundary layer or at the intersection of boundary layers in each of the four corners arising from non-isentropic turbulence. When the flow reaches the middle of the slice, flow structures in the order of the tube size have mostly disappeared. When the flow reaches the outlet, velocity vectors do not have noticeable secondary flow, although a small cross-stream velocity is still present.

Figure 11 shows similar results but at a plane in the machine direction. The creation of flow structures in the calming region is evident as the jets from each tube expand and interact. These structures are quickly dampened by the accelerating flow in the slice. The boundary layer is thin in the slice region because of the converging flow, except near the exit where the boundary layer is more noticeable. The contours show the velocity in the cross-machine direction. These contours indicate the strong effect the tubes have on the flow at the slice entrance. The decay and possible stretching of the flow structures is evident in Figure 12 where contours of velocities in the cross-machine direction, paper thickness direction, and machine direction are presented for various planes along the slice. The edge wall of the slice is on the right hand side in this figure.

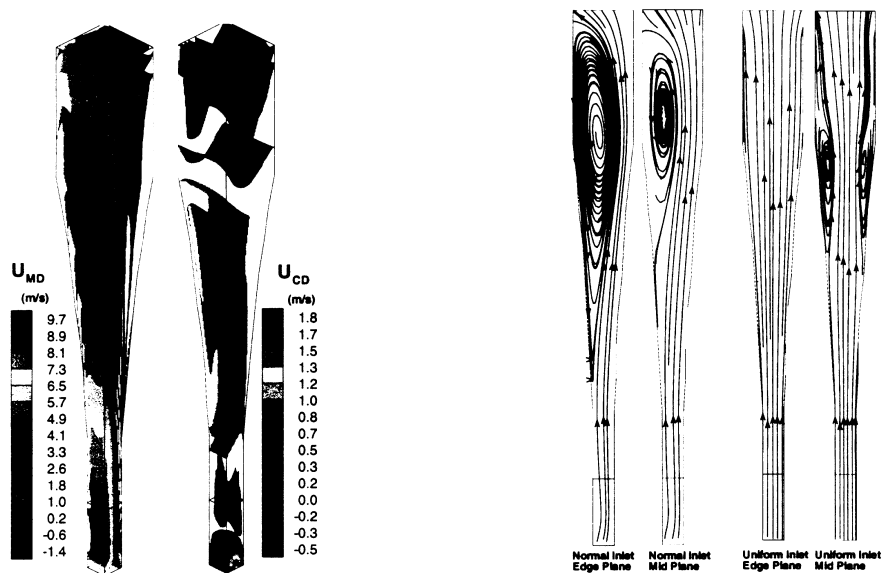


Figure 9: (a) Velocity contours in the cross-machine direction and machine direction in one of the diffuser tubes, and (b) Streamlines inside a diffuser tube at planes either near the wall or in the middle of the tube and for a uniform flow velocity imposed at the inlet of the tube and for a velocity distribution calculated from the complete headbox calculation

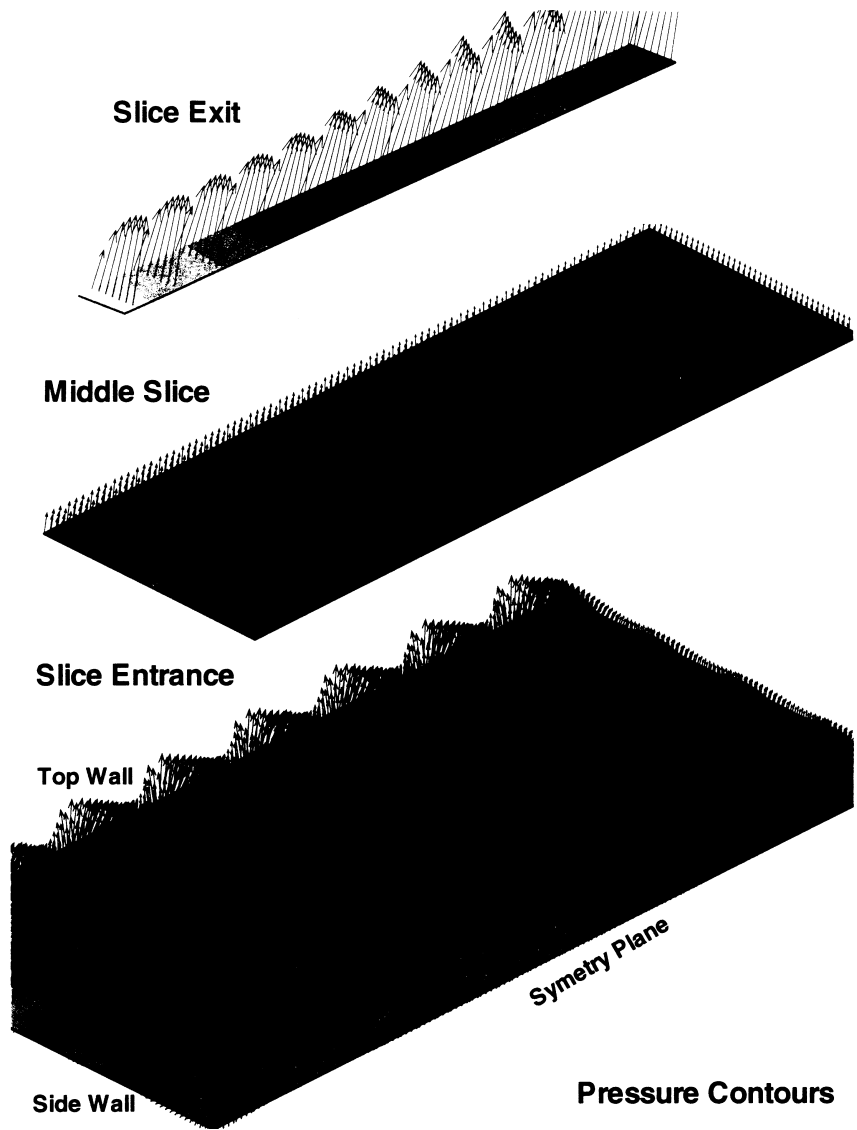


Figure 10: Velocity vectors at three planes normal to the slice with pressure contours corresponding to the area spanned by the first 8 columns of diffuser tubes and the first 4 rows

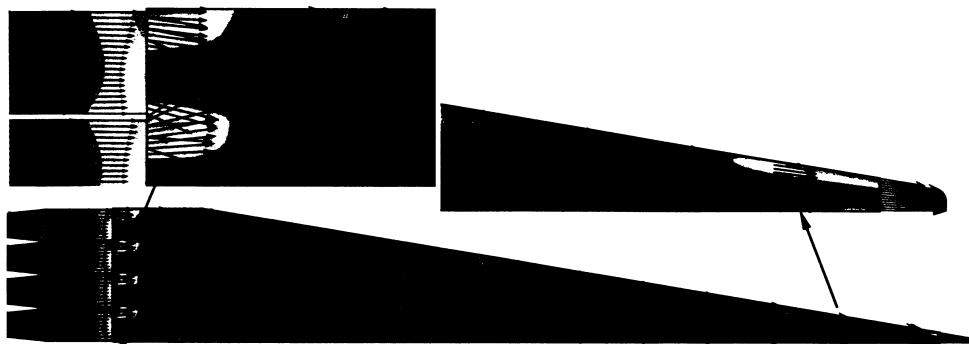


Figure 11: Velocity vectors and contours in the cross-machine direction in the slice and part of diffuser tubes

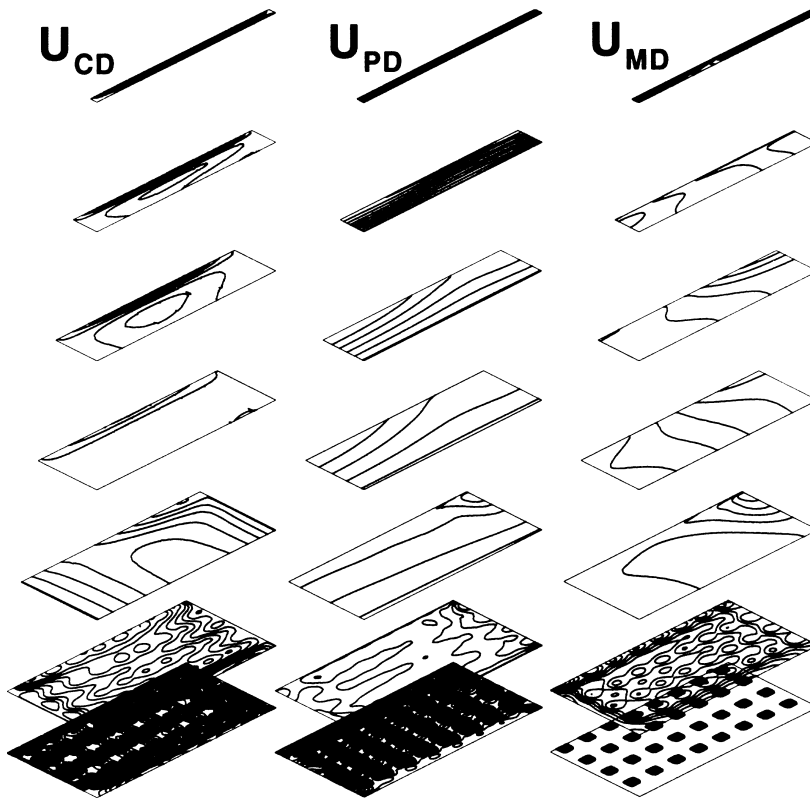


Figure 12: Velocity contours in the cross-machine direction, paper thickness direction, and machine direction corresponding to the area spanned by the first 8 columns of diffuser tubes and the first 4 rows

## CONCLUSIONS

A computational model is presented for the prediction of flow characteristics in a complete hydraulic headbox. The model uses block-structured curvilinear grids to allow the treatment of the complex geometry occurring in headboxes. The average velocity in each of the diffuser tubes is non-uniform in both the cross-machine direction and across rows of tubes. The cornering of the flow as it enters each diffuser tube causes a significant recirculation zone near the front wall of each tube. The exit flow from each diffuser tube is shown to be highly non-uniform with a significant degree of interaction as the flow proceeds into the slice. Computation of the headbox demonstrates that the method developed has the ability to model headboxes with complex geometries and has the potential to be an important and valuable analysis tool for the design and optimization of pulp and paper headboxes.

## ACKNOWLEDGMENTS

The authors would like to thank Weyerhaeuser for their interest and financial support. Funding from the Natural Sciences and Engineering Research Council of Canada and from Process Simulations Limited (PSL) is gratefully acknowledged.

## References

- [1] J. Mardon, E.G. Hauptmann, R.E. Monahan and E.S. Brown. The Extant State of the Manifold Problem. *Pulp & Paper Magazine of Canada*, 72(11):76–8, 1971.
- [2] A.D. Truffitt. Design Aspects of Manifold Type Flowspreaders. In *Pulp and Paper Technology Series*, TAPPI, 1975.
- [3] S. Syrälä, P. Saarenrinne and R. Karvinen. Fluid Dynamics of a Tapered Manifold Flow Spreader. In *TAPPI Engineering Conference*, pages 223–23, Chicago, Illinois, 1988.

- [4] G.L. Jones and R.J. Ginnow. Modeling Headbox Performance with Computational Fluid Mechanics. In *TAPPI Engineering Conference*, pages 15–20, Chicago, Illinois, 1988.
- [5] T. Shimizu and K. Wada. Computer Simulation of Measurement of Flow in a Headbox. In *Proceedings of the Pan Pacific Pulp and Paper Technology Conference*, pages 157–165, 1992.
- [6] J. Hämäläinen. Mathematical Modelling and Simulation of Fluid Flows in the Headbox of Paper Machines. Ph.D. Thesis, University of Jyväskylä, 1993.
- [7] P. Tarvainen, R.A.E. Mäkinen and J. Hämäläinen. Shape Optimization for Laminar and Turbulent Flows with Applications to Geometry Design of Paper Machines. Proceedings of the 10<sup>th</sup> International Conference on Finite Elements in Fluids, University of Arizona, pages 536–545, 1998.
- [8] J.J. Lee and S.B. Pantaleo. Headbox Flow Analysis. In 84<sup>th</sup> *Annual Meeting, Technical Section CPPA*, B339–B344, 1998.
- [9] C.K. Aidun and A. Kovacs. Hydrodynamics of the Forming Section: The Origin of Nonuniform Fiber Orientation. TAPPI 1994 Engineering Conference, Atlanta GA, 1994.
- [10] C.K. Aidun. Hydrodynamics of Streaks on the Forming Table. *TAPPI Journal*, 80(8):155–162, 1997.
- [11] L. Hua. Computational Modelling of a Manifold Type Flowspreader. Ma.Sc. Thesis, The University of British Columbia, 1998.
- [12] P. He and M. Salcudean. A Numerical Method for 3D Viscous Incompressible Flows Using Non-Orthogonal Grids. *Int. J. Numer. Meth. Fluids*, 18, 1994.
- [13] H. Pingfan, E.L. Bibeau, L. Hua, M. Salcudean and I. Gartshore. Fluid Dynamics of the Flow Distribution in a Headbox. Paper Presented at the CPPI Conference, Montreal, January 1998.